

Detection of α_2 -Adrenergic Receptors in Brain of Living Pig with ^{11}C -Yohimbine

Steen Jakobsen¹, Kasper Pedersen¹, Donald F. Smith², Svend B. Jensen¹, Ole L. Munk¹, and Paul Cumming¹

¹Aarhus University PET Centre and Centre for Functionally Integrative Neuroscience, Aarhus, Denmark; and ²Center for Basic Psychiatric Research, Psychiatric Hospital of Aarhus University, Risskov, Denmark

There have been few radiotracers for imaging adrenergic receptors in brain by PET, but none has advanced for use in human studies. We developed a radiosynthesis for the α_2 -adrenergic antagonist ^{11}C -yohimbine and characterized its binding in living pigs. As a prelude to human studies with ^{11}C -yohimbine, we determined the whole-body distribution of ^{11}C -yohimbine and calculated its dosimetry. **Methods:** Yorkshire \times Landrace pigs weighing 35–40 kg were used in the study. Baseline and post-challenge PET recordings of ^{11}C -yohimbine in pig brain were conducted for 90 min, concurrent with arterial blood sampling, and with yohimbine and RX821002 as pharmacologic interventions. ^{15}O -Water scans were performed to detect changes in cerebral perfusion. The PET images were manually coregistered to an MR atlas of the pig brain. Maps of the ^{11}C -yohimbine distribution volume ($[V_d]$ mL g^{-1}) in brain were calculated relative to the arterial input function. **Results:** Whole-body scans with ^{11}C -yohimbine revealed high accumulation of radioactivity in kidney, intestine, liver, and bone. The estimated human dose was 5.6 mSv/GBq, a level commonly accepted in human PET studies. Brain imaging showed baseline values of V_d ranging from 1.9 in medulla, 3.0 in cerebellum, and to 4.0 in frontal cortex. Coinjection with nonradioactive yohimbine (0.07 mg/kg) reduced V_d globally to approximately 1.5–2 mL g^{-1} . A higher yohimbine dose (1.6 mg/kg) was without further effect on self-displacement. Very similar results were obtained by displacement with the more selective α_2 -adrenergic antagonist RX821002 at doses of 0.15 and 0.7 mg/kg. Cerebral blood flow was globally increased 43% after administration of RX821002. Notable features of ^{11}C -yohimbine are a lack of plasma metabolism over 90 min and a rapid approach to equilibrium binding in brain. **Conclusion:** The new radiotracer ^{11}C -yohimbine seems well suited for PET investigations of α_2 -adrenergic receptors in brain and peripheral structures, with the caveat that displaceable binding was present in cerebellum and throughout the brain.

Key Words: adrenergic; receptors; yohimbine; RX821002; PET; receptor binding

J Nucl Med 2006; 47:2008–2015

Since the first report of external detection of dopamine D₂-like receptors in living brain (1), specific radioligands have

been developed for PET studies for receptors and reuptake sites of the biogenic amines dopamine, serotonin, and noradrenaline (2,3). Altered noradrenergic transmission is implicated in several neurodegenerative diseases and in the mechanism of action of some antidepressants. However, radiotracers for markers of noradrenaline innervations and receptors have become available only in recent years. Plasma membrane noradrenaline transporters on presynaptic terminals can now be imaged with ^{11}C -labeled 2-[(2-methoxyphenoxy)phenylethyl]morpholine (^{11}C -MeNER) (4). Whereas specific radiotracers are not available for imaging of brain β -adrenergic receptors, α_2 -adrenergic receptors in brain have been labeled with the antagonist ^{11}C -mirtazapine. However, that compound suffers from incomplete selectivity for adrenergic receptors (5). Therefore, a more specific marker for PET studies of α_2 -adrenergic receptors is required.

Yohimbine is the major alkaloid from the bark of *Pausinystalia yohimbe*, a West African plant, and is also present in extracts of *Rauwolfia* sp. Yohimbine has a long history as an antihypertensive agent but generally increases blood pressure at rest, apparently mediated by a central antagonism of α_2 -adrenergic receptors (6). In addition to α_2 -adrenergic antagonist properties, yohimbine interacts with α_1 and 5-hydroxytryptamine 1A (5-HT_{1A}) receptors (7–9). Despite the complex pharmacology of yohimbine, we hypothesized that ^{11}C -yohimbine at tracer concentrations might exhibit selectivity for α_2 -adrenergic sites in living brain. To test this hypothesis, we developed a radiosynthesis for ^{11}C -yohimbine and characterized its cerebral uptake and binding in PET studies of living pigs. The equilibrium distribution volume ($[V_d]$ mL g^{-1}) of ^{11}C -yohimbine was mapped in a baseline condition and after blockade with low and high doses of nonradioactive yohimbine. In other displacement studies, the pharmacologic specificity of ^{11}C -yohimbine for α_2 sites was tested by displacement with the selective α_2 antagonist RX821002 (9). We also determined the whole-body distribution of ^{11}C -yohimbine in a single pig and calculated organ dosimetry.

MATERIALS AND METHODS

Chemicals

Acetonitrile, dimethyl sulfoxide (DMSO), and iodine were from Bie & Berntsen. Yohimbine hydrochloride, yohimbinic acid,

Received Jul. 13, 2006; revision accepted Sep. 5, 2006.
For correspondence or reprints contact: Steen Jakobsen, PhD, PET Centre, Aarhus University Hospitals, Nørrebrogade 44, Aarhus C, Denmark 8000.
E-mail: steen@pet.auh.dk
COPYRIGHT © 2006 by the Society of Nuclear Medicine, Inc.

tetrabutylammonium fluoride (TBAF, 1 mol/L in tetrahydrofuran), and sodium phosphate monohydrate were from Sigma–Aldrich. RX821002 hydrochloride was from Tocris. Solutions for intravenous administrations of yohimbine (5% ethanol in sterile saline) and RX821002 (sterile saline) were prepared 30 min before use. The individual doses are expressed on the basis of the free base.

Radiochemistry

^{11}C -Carbon dioxide was prepared by $^{14}\text{N}(\text{p},\alpha)\text{C}$ proton bombardment with the GE Healthcare PETtrace 200 cyclotron and was converted to ^{11}C -methyl iodide using the GE Mel Box (reduction of CO_2 to CH_4 , followed by gas-phase reaction with iodine). ^{11}C -Methyl iodide (6–9 GBq after 30-min bombardment at 40 μA) was trapped in DMSO (300 μL) containing NaOH (1.5 μL , 3 mol/L), TBAF (5 μL , 1 mol/L), and yohimbic acid (1.5 mg) in a 1-mL vial. This mixture was heated at 90°C for 5 min. Purification of ^{11}C -yohimbine was performed by semipreparative high-performance liquid chromatography (HPLC) (PerkinElmer model 200) using a 5-mL injection loop. The mobile phase, consisting of 50% aqueous 70 mmol/L NaH_2PO_4 and 50% acetonitrile, was delivered at a rate of 8 mL/min to a Spherclone ODS(2) C-18 (Phenomenex, 250 \times 10 mm) semipreparative column. The reaction was quenched by adding 500 μL of HPLC eluent to the vial, and the mixture was transferred to the injection loop. Product elution was monitored with online γ -detection of an in-house design and ultraviolet (UV)–visible detection (model 759A, $\lambda = 254$ nm; Applied Biosystems). The fraction containing ^{11}C -yohimbine (retention time, 4–5 min) was collected and the mobile phase was removed by evaporating to near-dryness at 90°C under reduced pressure. The product was reformulated with isotonic saline and was transferred through a sterile filter (0.22 μm) to the final product vial. A small sample (100 μL) was taken for quality control measurement.

Analytic Chemistry

The amount of yohimbine in the final product was determined by HPLC using a LUNA CN 5- μm 100 column (Phenomenex, 250 \times 4.6 mm) with an eluent consisting of 60% aqueous 70 mmol/L Na_2HPO_4 and 40% acetonitrile with serial radioactivity and UV detection. Reference standards of yohimbic acid (5 $\mu\text{g}/\text{mL}$) and yohimbine (5 $\mu\text{g}/\text{mL}$) were used for quantification, and a solution of yohimbine (100 $\mu\text{g}/\text{mL}$) was coinjected with the product solution to verify product identity on the basis of the elution position of the UV peak. The chemical stability of ^{11}C -yohimbine productions was checked 1 h after the end of synthesis (EOS).

Biologic Procedures

This project was approved by The Danish Experimental Animal Inspectorate. Female pigs (Yorkshire \times Danish Landrace cross-bred, 35–40 kg) ($n = 7$) were prepared for scanning, as described in detail elsewhere (10). Anesthesia was induced with ketamine/midazolam and maintained with isoflurane/ $\text{N}_2\text{O}/\text{O}_2$. Body temperature and blood chemistry (gases, glucose, and pH) of the pigs were maintained within the normal range, and isotonic saline was infused intravenously at a rate of 3 mL/min. Heart rate, blood oxygen saturation, and arterial blood pressure were continuously monitored. Arterial blood samples were drawn every 1–2 h and levels of glucose, partial pressure of oxygen (P_{O_2}), partial pressure of carbon dioxide (P_{CO_2}), and pH were determined. Blood glucose levels were maintained within the normal porcine range of 3.5–6 mmol/L by intravenous infusion of isotonic glucose as required. Hemodynamic stability was maintained by adequate levels of

isoflurane anesthesia (i.e., 2%–2.5%). In addition, oxygen tension in the bloodstream was kept above 12 kPa, and CO_2 levels were maintained between 5.5 and 6.5 kPa by manual adjustments of respiration rate, respiratory volume, and the composition of the gaseous mixture delivered to the pig. Levels of pH in the bloodstream were maintained between 7.35 and 7.45 primarily by adjusting the tidal volume of gases delivered via the tracheal tube. After the last scan, pigs were killed with an overdose of pentobarbital.

Whole-Body PET Recording and Dosimetry Recordings

A whole-body PET recording of ^{11}C -yohimbine was performed in 1 pig using a Siemens ECAT EXACT HR47 tomograph. A whole-body transmission scan was obtained first. A series of 3 consecutive whole-body PET recordings were obtained after a single intravenous injection of ^{11}C -yohimbine (223 MBq; specific activity of 120 GBq/ μmol at time of injection). Seven horizontal bed positions were recorded at intervals of 2, 3, and 4 min; thus, the entire body was scanned during intervals of 0–14, 15–35, and 36–63 min after tracer injection.

Time–radioactivity curves were obtained from the repeated whole-body scans as follows: organs with relatively high accumulation of tracer relative to their surroundings were identified by visual inspection (bone, kidney, intestine, liver, and urinary bladder) and were included as individual source organs. Their tracer content was determined by extraction of the radioactivity concentration (Bq/mL) from a large volume of interest (VOI) defined in several consecutive transaxial planes through each organ. The measured concentrations were converted to total radioactivity content by multiplying by the relevant organ mass for the standard man (11) and dividing by the organ density. Because the urinary bladder was drained continuously during the PET procedure, the bladder radioactivity content was estimated from the difference between the injected dose and the decay-corrected total whole-body radioactivity. To estimate exposure after the last emission frame, the residual radioactivity was assumed to decrease thereafter only by physical decay. For each source organ, the percentage of injected dose (%ID) was plotted as a function of time, and the residence times were calculated as the areas under these curves from time zero to infinity.

Organ absorbed doses were based on the OLINDA/EXM scheme of a standard adult man, using the residence time of the source organs, calculated above. Results were multiplied by a correction factor (37/73.3), expressing the ratio of the pig body weight to that of the standard adult man. Thus, the dosimetry results in the pig were normalized to the expected human radiation doses. Finally, the doses for 25 target organs and the total effective dose were estimated using the OLINDA 1.0 software (12).

Dynamic Brain Imaging

Pigs ($n = 6$) were positioned with their head in the center of the field of view of the tomograph, with the head held in place using a custom-made holder. After a brief transmission scan, pigs underwent a series of 3 dynamic emission recordings initiated on intravenous bolus injection of ^{11}C -yohimbine (240–593 MBq) at intervals of 120 min (corresponding to 6 ^{11}C -half-lives). The dynamic ^{11}C -yohimbine emission recordings consisted of 26 frames increasing in duration from 15 s to 10 min, for a total of 90 min. Three pigs received ^{11}C -yohimbine first in a baseline condition, and again after challenges, first with a low dose (0.07 mg/kg) and then with a high dose (1.6 mg/kg) of yohimbine. Excess cold

yohimbine was delivered as a slow intravenous bolus infusion beginning 5 min before initiation of the dynamic (3-dimensional [3D]) PET recordings. Three other pigs received ^{11}C -yohimbine in a baseline condition, and again after challenge, first with a low dose (0.15 mg/kg) and then with a high dose (0.7 mg/kg) of RX821002, administered as a 5-min bolus infusion beginning 30 min before the initiation of dynamic (3D) PET recordings.

One yohimbine-challenged pig and all 3 RX821002-challenged pigs also underwent a series of 3-min, dynamic emission recordings (2-dimensional) after the administration of ^{15}O -water (500 MBq, intravenously), with continuous arterial sampling during the emission recording. Each ^{15}O -water scan was initiated 10 min before the ^{11}C -yohimbine scans, as described previously (13). In the present 4 animals with both baseline cerebral blood flow (CBF) and ^{11}C -yohimbine recordings, the blood-brain clearance of ^{11}C -yohimbine (K_1 , $\text{mL g}^{-1} \text{min}^{-1}$) was estimated by linear transformation of the first 3 min of the data recorded in cerebellum. The first-pass extraction fraction of ^{11}C -yohimbine was calculated relative to the CBF in the same animals as K_1/CBF .

Blood Chemistry and Metabolite Determination

During the dynamic ^{11}C -yohimbine recordings in baseline and under challenge conditions, a series of 40 blood samples were obtained from a femoral artery, at intervals increasing from 5 s to 10 min. Total plasma radioactivity was measured in a well counter cross-calibrated to the tomography. The fraction of untransformed ^{11}C -yohimbine was measured by radio-HPLC in extracts of plasma from samples taken at 2, 5, 10, 20, 40, 60, and 90 min after injection. Different HPLC conditions were tested: LUNA CN 5- μm 100 column (Phenomenex, 250×4.6 mm) with an eluent consisting of 60% aqueous 70 mmol/L Na_2HPO_4 and 40% acetonitrile; Spherclone Silica (Phenomenex, 250×4.6 mm) using 95% methanol and 5% acetic acid, pH 4, as eluent; and third, Spherclone ODS(2) C-18 (Phenomenex, 250×4.6 mm) and a mixture of acetonitrile and aqueous 70 mmol/L Na_2HPO_4 (60:40) as eluent. Detection consisted of serial UV detection ($\lambda = 254$ nm) and radiodetection.

Image Analysis

Voxel-wise parametric maps of the V_d (mL g^{-1}) of ^{11}C -yohimbine were calculated in the native space relative to the arterial input by the method of Turkheimer et al. (14). In this method, Akaike-weighted averages of the estimates for 1- and 2-tissue compartment models obtained by fitting linearized equations (15) were used for the voxelwise estimation of the magnitude of V_d without division. In addition, we calculated V_d using the graphical method of Logan with arterial input (16), omitting the data from the first 10 min of each PET recording. Maps of CBF were calculated using an in-house (NYFLOW) implementation of the 3-weighted integration method (17). The resultant blood flow images were blurred with a 1-mm filter (full width at half maximum) for optimizing visual appearance.

Individual summed emission images were inspected for evidence of movement during the 6-h scanning sessions. Because there was inconspicuous movement in any case, the sum of all emission frames from each PET session was calculated and was manually registered to the MR-based common stereotactic space for pig brain (18), using 9 degrees of freedom and rigid-body linear transformation. The inverse of the calculated transformation matrix was used to resample the statistically defined anatomic templates for 10 brain regions into the native space, for calculation

of the mean magnitude of ^{11}C -yohimbine V_d for each region in the parametric maps.

Statistics

We used multivariate ANOVA (SPSS PC+) to determine whether drug challenge with either yohimbine or RX821002 significantly altered V_d values of ^{11}C -yohimbine in porcine brain regions. A paired t test was used to determine whether the RX821002 challenge affected CBF values. Bonferroni correction was applied to determine whether V_d values of ^{11}C -yohimbine differed significantly between brain regions and whether CBF values differed significantly.

RESULTS

Radiolabeling of Yohimbine

The radiosynthesis of ^{11}C -yohimbine is depicted in Figure 1. The radiochemical purity of ^{11}C -yohimbine was >95%, and the radiochemical yield was 60%–85%, calculated on the basis of the collected ^{11}C -methyl iodide. In initial test productions using an excess of sodium hydroxide, the radiochemical yield was <25%, presumably due to product decomposition. The mean specific radioactivity of ^{11}C -yohimbine was 40 GBq/ μmol (range, 10–300 GBq/ μmol), and the final content of yohimbinic acid was <1 $\mu\text{g/mL}$. Individual batch productions of ^{11}C -yohimbine showed no alterations in appearance, pH, and chemical or radiochemical purity at 1 h after the EOS. The product ^{11}C -yohimbine was chemically stable for at least an hour after the EOS. The metabolite analysis of the plasma samples showed only a single radioactive species—namely, untransformed ^{11}C -yohimbine. Even at late time points, radioactive plasma metabolites were not detected.

Whole-Body Dosimetry

The summed whole-body PET recording of ^{11}C -yohimbine in pig is shown in Figure 2. Table 1 presents the calculated dosimetry for humans, based on the data obtained in pig. The main part of the radioactivity was present in liver, with smaller amounts in brain and skeleton.

Cardiovascular Effects of Drug Administrations

In the baseline condition for both groups of pigs with pharmacologic challenge, the mean heart rate was 110 min^{-1} , and the mean systolic and diastolic arterial blood pressures were 118 and 76 mm Hg, respectively. The low dose of yohimbine (0.07 mg/kg) was without effect on cardiovascular function, whereas the high dose of yohimbine

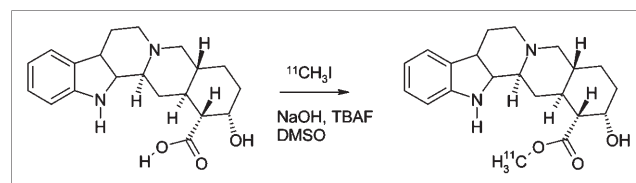


FIGURE 1. Radiosynthesis of ^{11}C -yohimbine from yohimbinic acid.

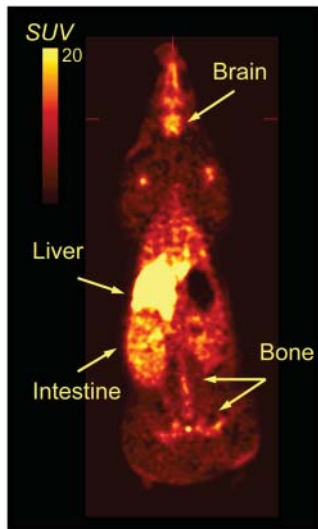


FIGURE 2. Whole-body distribution of ^{11}C -yohimbine in pig. Image is average of 3 consecutive whole-body scans. Standardized uptake value (SUV) is defined as percent radioactivity relative to injected dose divided by body weight.

(1.6 mg/kg) produced a transient 30% decrease in mean arterial blood pressure, associated with a 25% increase in heart rate, which, nonetheless, remained within the normal range for anesthetized pigs for the duration of the experiment. The RX821002 challenge at the low dose (0.15 mg/kg) produced an immediate 60% increase in heart rate that gradually returned to baseline values within 2 h, with no effect on mean arterial blood pressure; the high dose of RX821002 (0.7 mg/kg) had no further effect on heart rate.

Brain Imaging

Representative time–radioactivity curves measured in frontal cortex and cerebellum during 90 min after injection of ^{11}C -yohimbine in a baseline condition and after an intravenous bolus infusion of yohimbine (0.07 mg/kg) appear in Figure 3A. The radioactivity concentrations peaked at 15 min in cerebellum and at 25 min in frontal cortex, followed by a washout during the following 60 min. With RX821002 pretreatment, peak radioactivity concentrations occurred in cerebellum and frontal cortex at 8 min (Fig. 3B). The corresponding arterial input Logan plots at baseline, and after low-dose yohimbine challenge, are illustrated in Figure 3C, whereas the low dose of RX21002 is illustrated in Figure 3D.

In all brain regions and under all conditions, the mean voxelwise V_d values obtained by the Logan method were virtually identical to the results obtained by the method of Turkheimer et al. (14), the latter results are presented in Tables 2 and 3. The distribution of ^{11}C -yohimbine in the baseline condition showed regional differences; highest binding was found in cortical structures and thalamus, intermediate binding was in mesencephalon, and lowest binding was in cerebellum, pons, and medulla. Administration of yohimbine at 0.07 mg/kg decreased the magnitude of V_d in all brain regions to approximately 2 mL g^{-1}

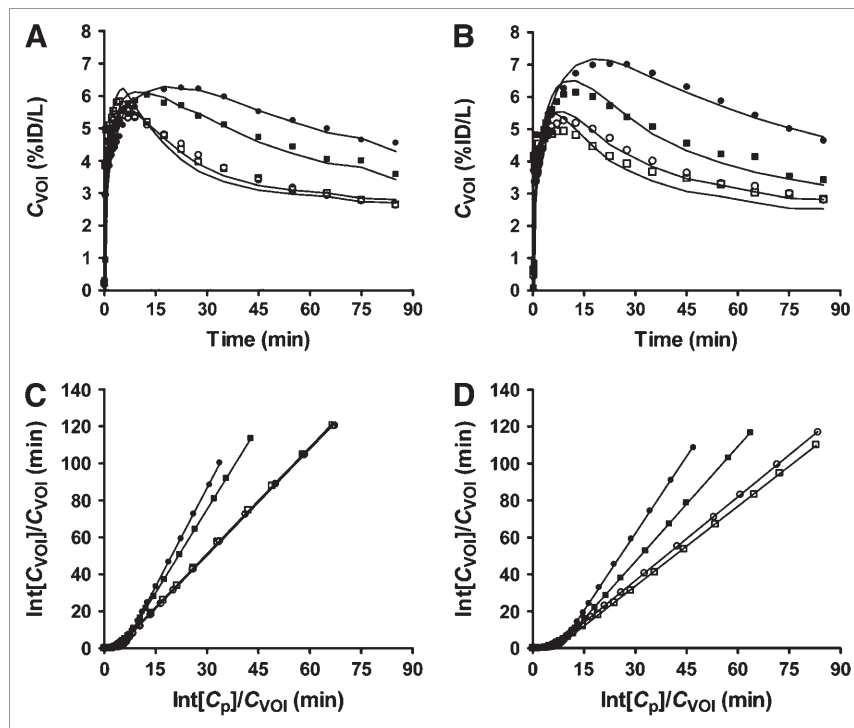
TABLE 1
Radiation Dose Estimates to Human Target Organs Based on Biodistribution Data from Pig Given Injection of ^{11}C -Yohimbine

Organ	Absorbed dose (mSv/GBq)
Adrenals	2.73
Brain	3.75
Breasts	1.54
Gallbladder wall	3.41
LLI wall	4.47
Small intestine	2.62
Stomach wall	2.15
ULI wall	3.98
Heart wall	2.19
Kidneys	5.87
Liver	12.3
Lungs	2.00
Muscle	2.09
Ovaries	3.09
Pancreas	2.62
Red marrow	2.14
Osteogenic cells	7.52
Skin	1.56
Spleen	2.00
Testes	2.34
Thymus	1.80
Thyroid	1.79
Urinary bladder wall	54.3
Uterus	4.39
Total body	2.69
Effective dose	5.66

LLI = lower large intestine; ULI = upper large intestine.

(Fig. 4). The repeated-measures data analysis indicated that challenge with yohimbine significantly reduced V_d values of ^{11}C -yohimbine in porcine brain (within-factor [scan], $P < 0.01$), with a generally greater decline in regions with relatively high baseline values than those with low values at baseline (scan \times region interaction, $P < 0.001$). In addition, regional V_d values of ^{11}C -yohimbine in pigs challenged with yohimbine tended to be lower in medulla and pons than in other brain regions (main effect of region, $P < 0.01$). The higher dose of yohimbine had no further effect on V_d ; slight increases relative to the low dose of yohimbine were not significant. The administration of RX821002 at the low dose evoked a uniform displacement of ^{11}C -yohimbine throughout the brain (Fig. 5), and the high dose was without further effect (Table 2). The repeated-measures data analysis indicated that challenge with RX821002 significantly reduced V_d values of ^{11}C -yohimbine in porcine brain (within-factor [scan], $P < 0.01$). Moreover, the decline in ^{11}C -yohimbine binding after challenge with RX821002 was generally greater in regions with relatively high baseline V_d values, such as thalamus and cortical regions, than in regions with relatively low baseline values (scan \times region interaction, $P < 0.001$).

FIGURE 3. Time-radioactivity curves and arterial input Logan plots of ^{11}C -yohimbine studied by PET in living porcine brain. Time-radioactivity measurements in frontal cortex (●) and cerebellum (■) in baseline condition, and in frontal cortex (○) and cerebellum (□) after challenge with low-dose yohimbine (A), and corresponding measurements before and after challenge with low-dose RX821002 (B) are presented along with fitting of a 1-compartment model to observed data (smooth lines). Corresponding arterial input Logan plots at baseline and after challenge with the low-dose yohimbine (C) and before and after challenge with low dose of RX821002 (D) are shown. Data are from representative experiment. C_{VOI} = radioactivity concentration in VOI; $\text{Int}[C_p]$ = integral of plasma radioactivity concentration.



Administration of 0.07 mg/kg yohimbine had no effect on CBF value, whereas the high dose of 1.6 mg/kg yohimbine resulted globally in a 30% reduction in CBF (data not shown). Pretreatment with the low dose of RX821002 evoked an increase in CBF in all brain regions examined (Fig. 5; Table 4; mean increase of $43\% \pm 8\%$). With regard to CBF, the data analysis indicated that RX821002 significantly increased values in porcine brain (within-subject factor [scan], $P < 001$), with the greatest change occurring in frontal cortex and putamen (scan \times region interaction, $P < 0.001$). However, no reliable overall difference was observed between brain regions in the effects of RX821002 on CBF values (main

effect of region, $P > 0.2$). No further increase was evoked by the high dose of RX821002. Baseline K_i for ^{11}C -yohimbine was $19 \pm 3 \text{ mL g}^{-1} \text{ min}^{-1}$ in cerebellum, corresponding to an extraction fraction of 27%.

DISCUSSION

Noradrenaline neurotransmission is implicated in brain functions such as attention, memory, and emotion (19,20). Abnormalities of noradrenaline function have been linked to several disorders such as anxiety and depression (21), and noradrenergic drugs have a long history as antidepressants

TABLE 2

Magnitude of V_d (mL/g) of ^{11}C -Yohimbine in Regions of Living Porcine Brain

Region	Baseline	Low-dose yohimbine (0.07 mg/kg)	High-dose yohimbine (1.6 mg/kg)
Cerebellum	3.20 ± 0.39	2.13 ± 0.41	2.18 ± 0.19
Medulla	2.06 ± 0.13	1.63 ± 0.27	1.71 ± 0.15
Mesencephalon	3.21 ± 0.17	2.30 ± 0.31	2.41 ± 0.18
Pons	2.74 ± 0.18	2.09 ± 0.29	2.19 ± 0.12
Thalamus	3.76 ± 0.38	2.55 ± 0.53	2.69 ± 0.30
Caudate	3.67 ± 0.57	2.40 ± 0.51	2.52 ± 0.23
Putamen	3.80 ± 0.43	2.47 ± 0.48	2.64 ± 0.28
Frontal cortex	4.01 ± 0.53	2.33 ± 0.55	2.28 ± 0.25
Temporal cortex	3.67 ± 0.50	2.27 ± 0.51	2.26 ± 0.21
Occipital cortex	3.63 ± 0.39	2.32 ± 0.46	2.32 ± 0.15

Values are mean \pm SD ($n = 3$).

TABLE 3

Magnitude of V_d (mL/g) of ^{11}C -Yohimbine Before and After Challenge with RX821002

Region	Baseline	Low-dose RX821002 (0.15 mg/kg)	High-dose RX821002 (0.7 mg/kg)
Cerebellum	2.66 ± 0.51	1.83 ± 0.35	2.07 ± 0.48
Medulla	1.87 ± 0.33	1.52 ± 0.24	1.74 ± 0.42
Mesencephalon	2.86 ± 0.57	1.94 ± 0.35	2.21 ± 0.53
Pons	2.42 ± 0.46	1.86 ± 0.34	2.08 ± 0.51
Thalamus	3.44 ± 0.66	2.12 ± 0.37	2.42 ± 0.57
Caudate	3.31 ± 0.54	2.03 ± 0.35	2.33 ± 0.49
Putamen	3.23 ± 0.44	2.07 ± 0.38	2.37 ± 0.55
Frontal cortex	3.51 ± 0.66	1.91 ± 0.35	2.16 ± 0.51
Temporal cortex	3.30 ± 0.67	1.91 ± 0.37	2.15 ± 0.51
Occipital cortex	3.21 ± 0.60	1.92 ± 0.33	2.15 ± 0.48

Values are mean \pm SD ($n = 3$).

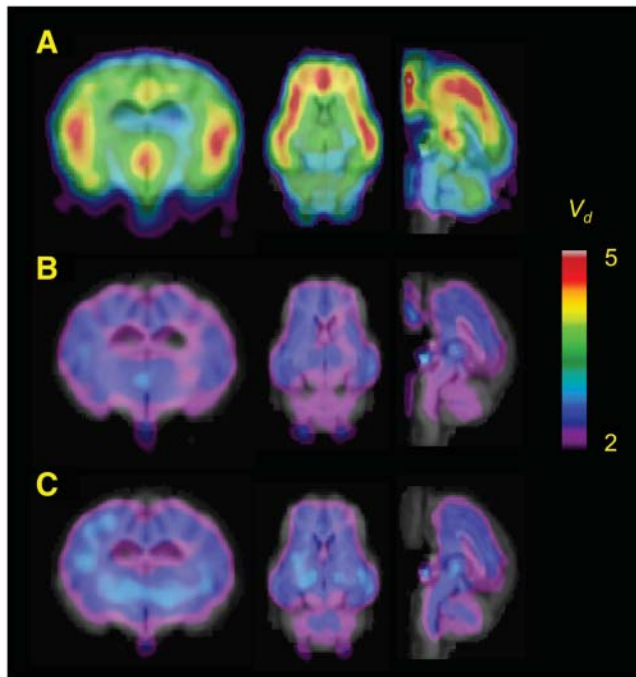


FIGURE 4. Parametric maps of ^{11}C -yohimbine in living porcine brain. Pharmacologic condition: (A) baseline; (B) 0.07 mg/kg yohimbine; (C) 1.6 mg/kg yohimbine. Each map is mean of 3 separate determinations, resampled into MR-based common stereotactic space for pig brain, and maps are shown superimposed on the MR image.

and antihypertensive agents. Some symptoms of acute withdrawal from opiates and alcohol are associated with overactivity of noradrenergic neurons in the locus coeruleus, a cell nucleus that may be altered by chronic cigarette smoking. Finally, loss of noradrenergic forebrain innerva-

tions has been noted in degenerative diseases such as Alzheimer's disease and multisystem atrophy (22,23), and inhibition of noradrenaline transporter has some efficacy in the treatment of Parkinson's disease (24).

The role of sympathetic innervations on the control of cerebral circulation has been extensively studied since the 1970s (25). In the present study, the α_2 -adrenoceptor antagonist RX821002 globally increased CBF by approximately 40%. We have reported a similar increase in CBF in pigs treated with mirtazapine (5). In contrast, the high dose of yohimbine in the present study tended to decrease the magnitude of CBF in the anesthetized pig, as we have observed earlier (5). Thus, reduced CBF evoked by a high dose of yohimbine may be attributable to effects mediated by cerebrovascular receptors other than α_2 -adrenergic receptors in pig brain. Contraction of cerebral arteries is mediated by α_2 -adrenergic receptors in dogs but by α_1 -adrenergic receptors in monkeys and humans (26). Thus, yohimbine at high doses may mediate a decrease in CBF in pig by a mechanism distinct from the increases evoked by mirtazapine and RX821002 by antagonism of α_2 -adrenergic sites. On the basis of the pharmacology of yohimbine, we speculate that this action is linked to α_1 -adrenergic binding sites.

The α_2 -adrenergic receptors have been described so far by autoradiography only in cerebellum of the pig (27). However, we have developed ^{11}C -mirtazapine for imaging studies of α_2 -adrenergic receptors in brain (5). ^{11}C -Mirtazapine, like ^{11}C -yohimbine in the present study, had notably high binding in the medial frontal and cingulate cortices of the pig, intermediate binding in the thalamus, and only traces of displaceable binding in the cerebellum, generally consistent with in vitro autoradiographic results

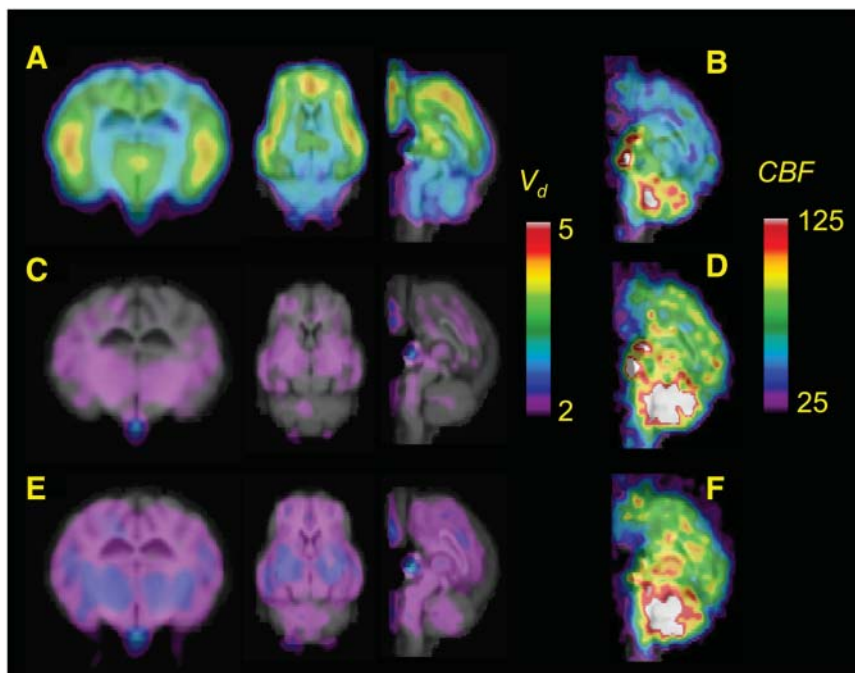


FIGURE 5. Parametric maps of ^{11}C -yohimbine and ^{15}O -water in living porcine brain. Pharmacologic condition: (A and B) baseline; (C and D) 0.15 mg/kg RX821002; (E and F) 0.7 mg/kg RX821002. Each map is mean of 3 separate determinations, resampled into MR-based common stereotactic space for pig brain, and maps are shown superimposed on MR image.

TABLE 4

Regional CBF Under Baseline Conditions and in Response to Increasing Doses of RX821002

Region	Baseline	RX821002 (0.15 mg/kg)	RX821002 (0.7 mg/kg)	% Increase in CBF*
Cerebellum	69 ± 18	94 ± 27	89 ± 20	36
Medulla	42 ± 14	56 ± 22	46 ± 19	33
Mesencephalon	61 ± 12	85 ± 16	85 ± 15	39
Pons	66 ± 17	85 ± 23	78 ± 21	29
Thalamus	58 ± 6	80 ± 10	85 ± 9	40
Caudate	52 ± 7	76 ± 11	81 ± 9	46
Putamen	50 ± 6	77 ± 11	77 ± 8	54
Frontal cortex	46 ± 7	68 ± 11	67 ± 13	48
Temporal cortex	43 ± 8	63 ± 13	60 ± 10	47
Occipital cortex	42 ± 10	60 ± 16	60 ± 15	43

*% increase between baseline and low-dose RX821002.

Values are expressed as mL/100 g/min and are mean ± SD (n = 3).

obtained for α_2 -adrenergic receptors for other species (28,29). However, displacement of ^{11}C -mirtazapine by yohimbine in living pig brain was incomplete; approximately 40% of the specific binding relative to cerebellum remained in diverse brain regions even after a high dose of nonradioactive yohimbine (3 mg/kg). Likewise, one third of ^{11}C -mirtazapine binding throughout pig brain was displaced by a low dose (0.1 or 1 mg/kg) of RX821002, suggesting that yohimbine and RX821002 have comparable affinity or selectivity toward α_2 -adrenoceptors. In contrast, ^{11}C -yohimbine binding was entirely and homogeneously self-displaced at a yohimbine dose of <0.1 mg/kg, indicating a very high-affinity interaction.

In spite of its long history of clinical use, there have been few studies reporting the metabolism of yohimbine in humans. We note both similarities and differences between yohimbine metabolism in humans and pigs. Le Corre et al. reported that the hepatic enzymes CYP3A4 and CYP2D6 degrade yohimbine to 10-hydroxy-yohimbine (10-OH YOH) and 11-hydroxy-yohimbine (11-OH YOH), with CYP2D6 playing the major role in the formation of 11-OH YOH (30), whereas no CYP2D6 activity could be detected in microsomes from pig liver (31). In addition, some individuals in the study of Le Corre et al. failed to form 11-OH YOH after injection of yohimbine. Similarly, no radioactive metabolites of yohimbine were found in plasma in the present pig study. In humans, 10-OH YOH is present in urine (32), whereas no studies of urinary metabolites have been performed yet in pigs. We view the lack of radioactive plasma metabolites of ^{11}C -yohimbine in pigs as convenient for quantification of α_2 -adrenoceptors by PET, but human studies may require more sophisticated kinetic models.

In anticipation of future human studies with ^{11}C -yohimbine, we have performed a whole-body dosimetry study. The whole-body distribution of ^{11}C -yohimbine is similar to

that of ^{11}C -mirtazapine in pig, and we estimate the human dose to be 5.6 mSv/GBq, which also compares with our earlier estimates for *rac*- ^{11}C -mirtazapine (6.8 mSv/GBq) and the (*S*-) and (*R*-) enantiomers (4.8–5.9 mSv/GBq) (6). Thus, we predict whole-body dosimetry in the range commonly accepted for neuroimaging in human subjects (33). However, radiation dose data extrapolated from pigs to humans may have underestimated the effective dose from ^{11}C -mirtazapine by 30%–35% (S.B. Hansen, unpublished data, September 2001). Consequently, we must measure whole-body dosimetry of ^{11}C -yohimbine in humans to fulfill requirements of radiation health authorities before using ^{11}C -yohimbine for PET neuroimaging in humans.

CONCLUSION

We have developed an efficient radiosynthesis for ^{11}C -yohimbine of high specific activity. The whole-body dosimetry study in pig suggests that this tracer could be safely used in human studies. Labeled ^{11}C -yohimbine metabolites were not detected in pig plasma, and the binding rapidly reached equilibrium in pig brain. The pattern of cerebral binding was consistent with the expected pig brain distribution of α_2 -adrenergic receptors. Binding of ^{11}C -yohimbine was entirely self-displaced by a very low dose of yohimbine or by a low dose of RX821002. We suggest that ^{11}C -yohimbine at tracer doses preferentially binds with high affinity to α_2 -adrenoceptors in brain and shows promise as a PET radioligand for in vivo studies.

ACKNOWLEDGMENTS

This work was supported by grants from Denmark's National Science Foundation and The Danish Medical Research Council.

REFERENCES

- Wong DF, Wagner HN Jr, Dannals R, et al. Effects of age on dopamine and serotonin receptors measured by positron tomography in the living human brain. *Science*. 1984;226:1393–1396.
- Frankle WG, Laruelle M. Neuroreceptor imaging in psychiatric disorders. *Ann Nucl Med*. 2002;16:437–446.
- Smith GS, Koppel J, Goldberg S. Applications of neuroreceptor imaging to psychiatry research. *Psychopharmacol Bull*. 2003;37:26–65.
- Schou M, Halldin C, Sovago J, et al. Specific in vivo binding to the norepinephrine transporter demonstrated with the PET radioligand, (*S,S*)-[^{11}C]MeNER. *Nucl Med Biol*. 2003;30:707–714.
- Smith DF, Dyve S, Minuzzi L, Jakobsen S, Munk OL, Cumming P. Inhibition of [^{11}C]mirtazapine binding by α_2 -adrenoceptor antagonists studied by positron emission tomography in living porcine brain. *Synapse*. 2006;59:463–472.
- Biaggioni I, Robertson RM, Robertson D. Manipulation of norepinephrine metabolism with yohimbine in the treatment of autonomic failure. *J Clin Pharmacol*. 1994;34:418–423.
- Newman-Tancredi A, Nicolas JP, Audinot V, et al. Actions of α_2 adrenoceptor ligands at α_{2A} and 5-HT $_{1A}$ receptors: the antagonist, atipamezole, and the agonist, dexmedetomidine, are highly selective for α_{2A} adrenoceptors. *Naunyn-Schmiedeberg's Arch Pharmacol*. 1998;358:197–206.
- Doxey JC, Lane AC, Roach AG, Virdee NK. Comparison of the α -adrenoceptor antagonist profiles of idazoxan (RX 781094), yohimbine, rauwolscine and corynanthine. *Naunyn-Schmiedeberg's Arch Pharmacol*. 1984;325:136–144.
- Clarke RW, Harris J. RX 821002 as a tool for physiological investigation of α_2 -adrenoceptors. *CNS Drug Rev*. 2002;8:177–192.

10. Poulsen PH, Smith DF, Ostergaard L, et al. In vivo estimation of cerebral blood flow, oxygen consumption and glucose metabolism in the pig by [¹⁵O]water injection. [¹⁵O]oxygen inhalation and dual injections of [¹⁸F]fluorodeoxyglucose. *J Neurosci Methods*. 1997;77:199–209.
11. Christy M, Eckerman K. *Specific Absorbed Fractions of Energy at Various Ages from Internal Photon Sources. I–VII*. ORNL/TM-8381 VI–V7. Oak Ridge, TN: Oak Ridge National Laboratory; 1987.
12. Stabin MG, Sparks RB, Crowe E. OLINDA/EXM: the second-generation personal computer software for internal dose assessment in nuclear medicine. *J Nucl Med*. 2005;46:1023–1027.
13. Cumming P, Rosa-Neto P, Watanabe H, et al. Effects of acute nicotine on hemodynamics and binding of [¹¹C]raclopride to dopamine D_{2,3} receptors in pig brain. *Neuroimage*. 2003;19:1127–1136.
14. Turkheimer FE, Hinz R, Cunningham VJ. On the undecidability among kinetic models: from model selection to model averaging. *J Cereb Blood Flow Metab*. 2003;23:490–498.
15. Zhou Y, Brasic JR, Ye W, et al. Quantification of cerebral serotonin binding in normal controls and subjects with Tourette's syndrome using [¹¹C]MDL 100,907 and (+)[¹¹C]McN 5652 dynamic PET with parametric imaging approach [abstract]. *Neuroimage*. 2004;22(suppl 2):T98.
16. Logan J, Fowler JS, Volkow ND, et al. Graphical analysis of reversible radioligand binding from time-activity measurements applied to [N-¹¹C-methyl]-(-)-cocaine PET studies in human subjects. *J Cereb Blood Flow Metab*. 1990;10:740–747.
17. Ohta S, Meyer E, Thompson CJ, Gjedde A. Oxygen consumption of the living human brain measured after a single inhalation of positron emitting oxygen. *J Cereb Blood Flow Metab*. 1992;12:179–192.
18. Watanabe H, Andersen F, Simonsen CZ, et al. MR-based statistical atlas of the Göttingen minipig brain. *Neuroimage*. 2001;14:1089–1096.
19. Smith A, Nutt D. Noradrenaline and attention lapses. *Nature*. 1996;380:291.
20. Smith AP, Wilson SJ, Glue P, Nutt DJ. The effects and after effects of the alpha₂-adrenoceptor antagonist idazoxan on mood, memory and attention in normal volunteers. *J Psychopharmacol*. 1992;6:376–381.
21. Nutt DJ, Pinder RM. α₂-Adrenoceptors and depression. *J Psychopharmacol*. 1996;10:35–42.
22. Gsell W, Jungkunz G, Riederer P. Functional neurochemistry of Alzheimer's disease. *Curr Pharm Des*. 2004;10:265–293.
23. Polinsky RJ. Multiple system atrophy: clinical aspects, pathophysiology, and treatment. *Neurol Clin*. 1984;2:487–498.
24. Takahashi H, Kamata M, Yoshida K, Higuchi H, Shimizu T. Remarkable effect of milnacipran, a serotonin-noradrenalin reuptake inhibitor (SNRI), on depressive symptoms in patients with Parkinson's disease who have insufficient response to selective serotonin reuptake inhibitors (SSRIs): two case reports. *Prog Neuropsychopharmacol Biol Psychiatry*. 2005;29:351–353.
25. Lluch S, Gomez B, Alborch E, Urquilla PR. Adrenergic mechanisms in cerebral circulation of the goat. *Am J Physiol*. 1975;228:985–989.
26. Toda N. Alpha adrenergic receptor subtypes in human, monkey and dog cerebral arteries. *J Pharmacol Exp Ther*. 1983;226:861–868.
27. Wikberg-Matsson A, Wikberg JE, Uhlen S. Identification of drugs subtype-selective for α_{2A}-, α_{2B}-, and α_{2C}-adrenoceptors in the pig cerebellum and kidney cortex. *Eur J Pharmacol*. 1995;284:271–279.
28. Strazielle C, Lalonde R, Hebert C, Reader TA. Regional brain distribution of noradrenaline uptake sites, and of alpha1-alpha2- and beta-adrenergic receptors in PCD mutant mice: a quantitative autoradiographic study. *Neuroscience*. 1999;94:287–304.
29. Young WS III, Kuhar MJ. Noradrenergic alpha 1 and alpha 2 receptors: light microscopic autoradiographic localization. *Proc Natl Acad Sci U S A*. 1980;77:1696–1700.
30. Le Corre P, Parmer RJ, Kailasam MT, et al. Human sympathetic activation by α₂-adrenergic blockade with yohimbine: bimodal, epistatic influence of cytochrome P450-mediated drug metabolism. *Clin Pharmacol Ther*. 2004;76:139–153.
31. Skaanild MT, Friis C. Characterisation of the P450 system in Göttingen minipigs. *Pharmacol Toxicol*. 1997;80(suppl 2):28–33.
32. Le Corre P, Dollo G, Chevanne F, Le Verge R. Biopharmaceutics and metabolism of yohimbine in humans. *Eur J Pharm Sci*. 1999;9:79–84.
33. Mejia AA, Nakamura T, Masatoshi I, Hatazawa J, Masaki M, Watanuki S. Estimation of absorbed doses in humans due to intravenous administration of fluorine-18-fluorodeoxyglucose in PET studies. *J Nucl Med*. 1991;32:699–706.